

# RNA guanine-7 methyltransferase catalyzes the methylation of cytoplasmically recapped RNAs

Jackson B. Trotman<sup>1,2,3</sup>, Andrew J. Giltmier<sup>1,3</sup>, Chandrama Mukherjee<sup>1,3</sup> and Daniel R. Schoenberg<sup>1,3,\*</sup>

<sup>1</sup>Center for RNA Biology, The Ohio State University, Columbus, OH 43210, USA, <sup>2</sup>Ohio State Biochemistry Program, The Ohio State University, Columbus, OH 43210, USA and <sup>3</sup>Department of Biological Chemistry and Pharmacology, The Ohio State University, Columbus, OH 43210, USA

Received April 19, 2017; Revised August 24, 2017; Editorial Decision August 25, 2017; Accepted August 30, 2017

## ABSTRACT

**Cap homeostasis is a cyclical process of decapping and recapping that impacts a portion of the mRNA transcriptome. The metastable uncapped forms of recapping targets redistribute from polysomes to non-translating mRNPs, and recapping is all that is needed for their return to the translating pool. Previous work identified a cytoplasmic capping metabolon consisting of capping enzyme (CE) and a 5'-monophosphate kinase bound to adjacent domains of Nck1. The current study identifies the canonical cap methyltransferase (RNMT) as the enzyme responsible for guanine-N7 methylation of recapped mRNAs. RNMT binds directly to CE, and its presence in the cytoplasmic capping complex was demonstrated by pulldown assays, gel filtration and proximity-dependent biotinylation. The latter also identified the RNMT cofactor RAM, whose presence is required for cytoplasmic cap methyltransferase activity. These findings guided development of an inhibitor of cytoplasmic cap methylation whose action resulted in a selective decrease in levels of recapped mRNAs.**

## INTRODUCTION

The 5' end of every mRNA is modified by addition of an N7-methylguanosine (m<sup>7</sup>G) cap that is required for proper mRNA processing and function (1). Until recently, the prevailing view was that mRNA capping is confined to the nucleus, that loss of the cap in the cytoplasm is irreversible and that uncapped 5' ends are rapidly degraded by Xrn1. The first evidence to the contrary came with the identification of stable decay intermediates of nonsense-containing β-globin mRNA in the cytoplasm of erythroid cells from transgenic

mice. These 5'-truncated RNAs are polyadenylated (2), and recent work showed they are generated by SMG6 cleavage of the nonsense-containing mRNA (3). Unexpectedly, the shortened transcripts were also modified on their 5' ends by a cap or cap-like structure (4). The mechanism responsible for this modification was unknown at the time; however, in confirming the m<sup>7</sup>G cap status of these RNAs, we identified a cytoplasmic pool of capping enzyme (CE; alternatively, RNGTT) that co-purifies with a 5' monophosphate RNA kinase (5' kinase) activity that generates diphosphate ends necessary for guanylate transfer by CE (5). The existence of cytoplasmic machinery capable of recapping 5' monophosphate ends suggested that decapping (and/or endonucleolytic cleavage) does not invariably lead to complete degradation and can instead generate substrates for subsequent recapping. We identified a number of recapping targets by their accumulation with uncapped 5' ends when cytoplasmic capping was inhibited by overexpression of a catalytically inactive, cytoplasmically restricted form of CE (6). Capped Analysis of Gene Expression (CAGE) performed as part of ENCODE provided additional evidence for cytoplasmic capping by identifying capped ends that do not map to transcription start sites but instead map to sites within spliced exons (7). It is estimated that these downstream cap sites account for 25% of capped ends (8), and a number of these capped ends were recently shown to map to the 5' ends of recapped transcripts (9). Cytoplasmic capping targets undergo a cyclical process of decapping and recapping, termed cap homeostasis, that impacts the translation of a subset of the mRNA transcriptome (6). When cytoplasmic capping is blocked, these transcripts move from polysomes to non-translating mRNPs, where they accumulate in a stable yet uncapped form. Importantly, these non-translating transcripts are polyadenylated, and the length of their poly(A) tails is sufficient to facilitate translation initiation after recapping (10).

\*To whom correspondence should be addressed. Tel: +1 614 688 3012; Fax: +1 614 292 3448; Email: schoenberg.3@osu.edu

Present address: Chandrama Mukherjee, Department of Life Sciences, Presidency University, Kolkata 700073, India.

**Disclaimer:** The content is solely the responsibility of the authors and does not necessarily represent the official views of Pelotonia, the Ohio State University, the American Heart Association or the National Institutes of Health.

Nuclear capping involves three successive reactions that are catalyzed by two enzymes, CE and RNA guanine-7 methyltransferase (RNMT). CE converts the 5'-triphosphate end of the nascent transcript to a 5'-diphosphate and then transfers GMP bound covalently at lysine 294 onto this. Synthesis of the basic cap structure (cap 0) is completed by methylation at N7 of the transferred guanosine by RNMT, and both CE and RNMT are juxtaposed to the nascent 5' end by binding to the C-terminal domain of RNA polymerase II. Cytoplasmic capping also involves three successive reactions but differs from nuclear capping by the process that generates the 5'-diphosphate intermediate. In cytoplasmic capping, the recapping substrate is generated by transfer of the  $\gamma$ -phosphate of ATP onto a 5'-monophosphate end by a polynucleotide 5'-monophosphate kinase. Mutual binding to the cytoplasmic adapter protein Nck1 (11) brings the 5' kinase and CE together in a single complex. Nck1 consists of three SH3 domains and a C-terminal SH2 domain. The 5' kinase binds to the second SH3 domain, and CE binds to the third SH3 domain through its proline-rich C-terminus. This organization of sequential enzymes in a metabolic pathway into a supramolecular complex, or metabolon, allows effective transport of substrates from one active site to the next and enhances the rate of catalysis by increasing the local concentration of substrates for downstream enzymes (12,13). Overexpression of forms of Nck1 that are unable to bind CE or the 5' kinase caused uncapped forms of recapping targets to accumulate (11), thus establishing the cytoplasmic capping complex as a metabolon that recaps 5' monophosphate ends. Echoing the multifunctionality of the cytoplasmic capping complex, trypanosomes have a cytoplasmic, bifunctional enzyme with 5' monophosphate kinase and guanylyltransferase activities that may likewise facilitate translational control through recapping (14).

The majority of translation is directed by the cap-binding translation initiation factor eIF4E, which, through the eIF4F complex, ultimately recruits the small ribosomal subunit to the mRNA 5' end (15). In order for recapped mRNAs to recapitulate the behavior of nuclear capped transcripts, the added cap guanosine must undergo N7 methylation. In the crystal structure of eIF4E, the cap guanine base is recognized by sandwich-stacking between two tryptophan side chains. Binding is strengthened by cation- $\pi$  interactions with the N7-methylguanine (16,17), such that the affinity of eIF4E for the m<sup>7</sup>G cap is three to four orders of magnitude stronger than that for the unmethylated equivalent. Guanine-N7 methylation is also needed to maintain mRNA stability in the presence of surveillance mechanisms that degrade mRNAs with improperly methylated caps (18,19).

The current study sought to identify the source of cytoplasmic cap methylation. Nuclear cap methylation is a regulated process (20) in which RNMT activity is stimulated by the binding of RNMT-activating miniprotein (RAM) to its C-terminal catalytic domain (21) and inhibited by loss of RAM (22). Regulation of RNMT and RAM by site-specific phosphorylation points to cap methylation as an evolving nexus of post-transcriptional control. Results presented here identify a cytoplasmic pool of RNMT, show this is a component of the cytoplasmic capping complex, and

demonstrate its function as the methyltransferase that catalyzes the final maturation step in cap homeostasis.

## MATERIALS AND METHODS

### Cell lines and cell culture

Human osteosarcoma (U2OS) cells obtained from ATCC (HTB-96) were cultured in McCoy's 5A medium (Thermo Fisher 116600–108) supplemented with fetal bovine serum (FBS) to 10% (v/v). Human embryonic kidney (HEK293) cells were cultured in Dulbecco's Modified Eagle Medium (Thermo Fisher 11995–073) supplemented with FBS to 10% (v/v). Cells were maintained at 37°C under 5% CO<sub>2</sub> and were discarded after no more than 20 passages.

### Transfection and subcellular fractionation

Prior to transfection, cells were given fresh, pre-warmed medium. HEK293 cells were 60–70% confluent at time of transfection with 10  $\mu$ g plasmid DNA per 10-cm dish using jetPRIME transfection reagent (Polyplus 114–15) according to manufacturer's protocol. Cells were cultured 24 or 48 h before being harvested. U2OS cells were 70–75% confluent at time of transfection with 6  $\mu$ g plasmid DNA per 10-cm dish using FuGENE 6 transfection reagent (Promega E2691) according to manufacturer's protocol. These cells were then cultured 24 h before being harvested. One 10-cm dish of U2OS cells was used per siRNA treatment. At the time of the first siRNA transfection, cells were 50% confluent. siRNA transfection mixtures were prepared with jetPRIME transfection reagent (Polyplus) and added to culture medium to bring siRNA to a concentration of 10 nM. After 24 h, the culture medium was removed, and the same procedure was repeated for a second transfection. After another 24 h, the cells were harvested. Trilencer-27 siRNAs (OriGene) used in this study are as follows: universal scrambled control siRNA (SR30004), RNMT siRNA (SR305750B), RAM siRNA (SR313193A). To harvest, cells were washed with phosphate-buffered saline (PBS) and then scraped into 1 ml PBS. After centrifugation at 70  $\times$  g for 10 min at 4°C, pellets were resuspended in 5–10 volumes of ice-cold YO Lysis Buffer (10 mM HEPES pH 7.3, 10 mM KCl, 10 mM MgCl<sub>2</sub>, 0.2% (v/v) IGEPAL CA-630, 2 mM dithiothreitol (DTT), 0.5 mM PMSF, 7.5  $\mu$ l/ml protease inhibitor cocktail (Sigma P8340), 7.5  $\mu$ l/ml phosphatase inhibitor cocktail 2 (Sigma P5726), 7.5  $\mu$ l/ml phosphatase inhibitor cocktail 3 (Sigma P0044)) by pipetting 10 times. Resuspended cells were incubated on ice for 10 min, pipetted five times, and centrifuged at 16 100  $\times$  g for 10 min at 4°C. The supernatants (cytoplasmic extracts) were removed and kept on ice. Residual supernatants were completely removed from the nuclear pellets before resuspending in 4–10 cell-pellet volumes of ice-cold YO Buffer A (10 mM HEPES pH 7.3, 25% (v/v) glycerol, 420 mM NaCl, 1.5 mM MgCl<sub>2</sub>, 0.2 mM ethylenediaminetetraacetic acid (EDTA), 1 mM DTT, 0.5 mM PMSF, 7.5  $\mu$ l/ml protease inhibitor cocktail (Sigma), 7.5  $\mu$ l/ml phosphatase inhibitor cocktail 2 (Sigma), 7.5  $\mu$ l/ml phosphatase inhibitor cocktail 3 (Sigma)) by pipetting 15 times. This was incubated end-over-end for 20 min at 4°C and then centrifuged (16

100 × *g* for 5 min at 4°C) to pellet nuclear debris. Supernatants (nuclear extracts) were removed and kept on ice. Total protein concentration in each extract was determined by Bradford assay using Bio-Rad Protein Assay Dye Reagent (Bio-Rad 5000006) normalized against a standard curve of BSA (Fisher Scientific BP1600–100). For cap methyltransferase activity assays, nuclear and cytoplasmic extracts were brought to the same protein concentration and buffer composition (Combo Buffer) by diluting to 50% with YO Lysis Buffer or YO Buffer A, respectively, and stored in small aliquots at –80°C. For sodium dodecyl sulfate-polyacrylamide gel electrophoresis (SDS-PAGE) analysis, extracts were diluted to 75% with 4× Laemmli Sample Buffer.

### Immunoprecipitation

Nuclear and cytoplasmic extracts corresponding to the same mass of protein (1000 µg for Figure 1B, 125 µg for Figure 4C) were brought to 500 µl under the same buffer composition (Combo Buffer) and pre-cleared with 15 µl slurry-equivalent of Dynabeads Protein G (Thermo Fisher 10003D) at 4°C for 45 min with end-over-end rotation. At the same time, 15 µl slurry-equivalent Dynabeads Protein G was incubated with 2 µg antibody in 500 µl Combo Buffer (for each immunoprecipitation) at 25°C for 45 min. Pre-cleared extract samples were then incubated with bead-bound antibodies end-over-end at 4°C overnight. Beads were washed three times with 500 µl Combo Buffer, 10 min end-over-end at 4°C per wash. Beads were resuspended in 20 µl Combo Buffer; a portion of this mixture was brought to 1× Laemmli Sample Buffer for SDS-PAGE, and the remaining mixture was stored in small aliquots at –80°C for cap methyltransferase activity assays.

### Generation of GpppRNA substrate for cap methyltransferase activity assay

*In vitro* transcription with the MEGAscript T3 Transcription Kit (Ambion 1138) was used to produce a 32-nt 5'-triphosphate RNA (pppRNA) with the same sequence as that used in (23). pppRNA was purified using a NucAway Spin Column (Thermo Fisher AM10070) and stored at –20°C. To generate radiolabeled GpppRNA, a 40-µl *in vitro* capping reaction was prepared, containing 10 mM Tris-HCl pH 7.5, 3 mM MgCl<sub>2</sub>, 1 mM DTT, 0.1 mM EDTA, 20% (v/v) glycerol, 24 pmol pppRNA, 24 pmol [ $\alpha$ -<sup>32</sup>P]GTP (3000 Ci/mmol, PerkinElmer BLU006H250UC) and 2 pmol recombinant His-CE. This reaction was incubated for 3 h at 30°C and then heat-inactivated for 10 min at 65°C. RNA was purified using the RNA Clean & Concentrator-5 kit (Zymo Research R1016), eluting with 30 µl RNase-free water. Yield of purified radiolabeled GpppRNA was measured by scintillation counting relative to input.

### Cap methyltransferase activity assay

Reactions were prepared, each containing 5 fmol radiolabeled GpppRNA, 50 mM Tris pH 8.0, 6 mM KCl, 1.25 mM MgCl<sub>2</sub>, 100 nM S-adenosylmethionine, 2 mM DTT and 20

U SUPERase-In (Thermo Fisher AM2696). Each reaction volume was 10 µl and contained either 4 µg (Figure 1B) or 1 µg (Figures 1D, 4E and 5C) nuclear or cytoplasmic extract, 1 µl immunoprecipitated (5% of total) bead slurry (Figure 1B), or 4 µl gel filtration fraction (Figure 2B). Reactions were incubated for 30 min at 37°C, and RNA was then immediately purified using the RNA Clean & Concentrator-5 kit (Zymo Research), eluting with 7 µl RNase-free water. Purified RNA was digested in a 7-µl reaction containing 5 µl purified RNA, 50 mM sodium acetate pH 5.2 and 0.44 U nuclease P1 (US Biological N7000). After incubating for 30 min at 37°C, 2 µl of each reaction was spotted on the origin of a pre-run PEI cellulose thin-layer chromatography plate (Macherey-Nagel 801053), which was then developed in 0.4 M ammonium sulfate. After overnight exposure to a storage phosphor screen, images were obtained with a Typhoon 9200 (Amersham).

### Streptavidin pulldown

HEK293 cells were transiently transfected with pQCXIP-MS2-bio or pcDNA3-bio-myc-NES-mCE ΔNLS (Figure 2C) or a 1:1 (w/w) ratio of pcDNA3-bio-myc-mCE with pcDNA4/TO-myc-GFP-FLAG, pcDNA3-FLAG-RNMT, pcDNA3-FLAG-RNMT 1–120 or pcDNA3-FLAG-RNMT 121–476 (Figure 2F). Prior to harvesting, cells for Figure 2F were incubated for 10 min at room temperature in PBS containing 0.15% formaldehyde before adding glycine (in PBS) to 115 mM, mixing well, and allowing incubation for 5 min at room temperature to quench free formaldehyde. Cytoplasmic extracts were prepared, and protein concentrations were measured. Equivalent protein amounts of each cytoplasmic extract were brought to 500 µl with YO Lysis Buffer, and concentrated NaCl solution was added to a final concentration of 150 mM. To each sample, 50 µl pre-equilibrated slurry-equivalent MyOne Streptavidin T1 Dynabeads (Thermo Fisher 65601) was added. Samples were incubated end-over-end at 4°C for 2 h before washing the protein-bound beads four times with 500 µl PD Buffer (YO Lysis Buffer containing 150 mM NaCl) at 4°C for 10 min. Beads were resuspended in 30 µl 2× Laemmli Sample Buffer for analysis by SDS-PAGE and western blot.

### GST pulldown

To 5 µg bead-bound GST or GST-RNMT, 30 µl glutathione Sepharose 4B beads (GE Healthcare) was added to better visualize the bead pellets. The bead mixtures were equilibrated in PD Buffer and then resuspended in 500 µl PD Buffer containing 1 µg His-CE. The mixtures were incubated end-over-end at 4°C for 2 h and then washed four times with 500 µl PD Buffer at 4°C for 10 min each. Beads were resuspended in 15 µl 2× Laemmli Sample Buffer and analyzed alongside an input sample by SDS-PAGE and western blot.

### Proximity-dependent biotinylation

Triplicate cultures of HEK293 cells were transiently transfected with a 1:3 (w/w) ratio of pcDNA3-FLAG-

RNMT and either pcDNA3.1-myc-BirA\* or pcDNA3.1-myc-BirA\*-cCE. After 6 h, a stock solution of 10 mM biotin (Sigma-Aldrich B4639-1G) in dimethylsulfoxide was prepared and added directly to medium to final concentrations of 0, 5 and 25  $\mu$ M biotin. Additional DMSO was added where necessary to normalize the volume of mix added to each dish. Cells were incubated 14 h before harvesting and preparing cytoplasmic extracts as described above. Streptavidin pulldown was performed as described above, using 300  $\mu$ g total cytoplasmic protein. Beads were resuspended in Laemmli Sample Buffer and analyzed by SDS-PAGE and western blot. Using the same cytoplasmic extracts, anti-FLAG immunoprecipitation was performed as described above for Figure 3B, except that the binding and washing steps used PD Buffer instead of Combo Buffer.

### Preparation of cytoplasmic RNA

Triplicate cultures of U2OS cells were transiently transfected with a 1:9 ratio (w/w) of pECE-EGFP-bio and either empty pcDNA3 or pcDNA3-FLAG-NES-RNMT 121–476 D203A. After 24 h, cells were harvested, and nuclear and cytoplasmic extracts were prepared, with the YO Lysis Buffer being supplemented with RNaseOUT (Thermo Fisher 10777019) to 0.4 U/ $\mu$ l. Total cytoplasmic RNA was prepared from cytoplasmic extracts using the Direct-zol RNA MiniPrep Kit (Zymo Research R2053) according to manufacturer's protocol, including on-column DNase I digestion. Purity and concentration of the prepared RNA were measured with a NanoDrop ND-1000 spectrophotometer.

### Recovery of capped RNA with GST-eIF4E

For each pulldown, 8  $\mu$ l slurry-equivalent Glutathione MagBeads (GenScript L00327) was equilibrated in Cap PD Buffer (150 mM NaCl, 0.1% (v/v) IGEPAL CA-630, 10 mM Tris pH 7.5, 1 mM DTT) before resuspending beads in 200  $\mu$ l Cap PD Buffer with 4  $\mu$ g GST-eIF4E K119A. Mixtures were incubated end-over-end at 4°C for 70 min, and then beads were washed five times with 200  $\mu$ l Cap PD Buffer. RNA mixtures of 400  $\mu$ l were prepared for each pulldown, each containing 1  $\mu$ g cytoplasmic RNA, 0.04 ng G-capped luciferase RNA and 80 U RNaseOUT (Thermo Fisher) in Cap PD Buffer. Washed protein-bound beads were resuspended in 200  $\mu$ l RNA mixtures, and the remaining 200  $\mu$ l RNA mixtures were kept on ice for analysis as input samples. Bead-RNA mixtures were incubated end-over-end at 4°C for 2 h, and the beads were then washed thrice with 200  $\mu$ l Cap PD Buffer at 4°C for 10 min. Washed beads were resuspended in 200  $\mu$ l Cap PD Buffer. RNA from each 200  $\mu$ l input and eIF4E-bound sample was purified using the Direct-zol RNA MiniPrep Kit (Zymo Research), eluting with 25  $\mu$ l RNase-free water.

### Quantitative reverse transcription PCR

To 0.5  $\mu$ g cytoplasmic RNA spiked with 0.02 ng luciferase RNA (Figure 5E) or 10  $\mu$ l purified input or eIF4E-bound RNA (Figure 5F), 100 ng random hexamers and 10 nmol each dNTP was added to a total volume of 13  $\mu$ l. Mixtures

were incubated at 65°C for 5 min and immediately placed on ice. Mixtures were brought to 20- $\mu$ l reverse transcription reactions containing 1 $\times$  First Strand Buffer, 5 mM DTT, 40 U RNaseOUT (Thermo Fisher) and 200 U SuperScript III reverse transcriptase (Thermo Fisher 18080044). Reactions were placed on a thermocycler with the following program: 25°C for 5 min, 50°C for 60 min, 70°C for 15 min. The resulting cDNAs were analyzed by quantitative reverse transcription PCR in triplicate 10- $\mu$ l reactions containing 0.5  $\mu$ M forward and reverse gene-specific primer (see Supplementary Table S2) and 1 $\times$  SensiFAST SYBR No-ROX mix (Bioline BIO-98020) with a Bio-Rad CFX Connect real-time PCR detection system. PCRs were performed with the program: 95°C for 3 min, 40 cycles of (95°C for 10 s, 55°C for 30 s).

### Quantification and statistical analysis

Cap methyltransferase activity data (Figures 1B, D, 2D, 4E and 5C) were quantified using ImageQuant TL software (GE Healthcare) to determine relative amounts of GpppG and m<sup>7</sup>GpppG for each sample. GraphPad Prism 6 software was used to conduct ratio paired (Figures 1D and 4E) and unpaired two-tailed (Figure 5C) *t*-tests to analyze independent biological triplicate experiments. Results with *P* < 0.05 were considered significant. RT-qPCR data (Figure 5E and F) were analyzed using Bio-Rad CFX Manager 3.1 software. Cq-values were determined by regression mode. For Figure 5E, the  $\Delta\Delta$ Cq method was used to calculate relative mRNA quantities among the samples for each gene, normalized to the luciferase spike control and to the non-recapping-target internal control BOP1. Normalized quantities were arbitrarily set to 1 for the vector control treatment. For Figure 5F, the  $\Delta$ Cq method was used to calculate relative mRNA quantities among the samples for each gene, and the technical mean quantity of each gene in the eIF4E-bound samples was normalized to the corresponding input quantity. The mean of independent biological replicates was presented  $\pm$  SEM using GraphPad Prism 6 software, and unpaired two-tailed *t*-tests were performed for each gene to compare vector control and  $\Delta$ N-RNMT samples. Results with *P* < 0.05 were considered significant.

Additional information can be found in Supplementary Materials and Methods.

## RESULTS

### RNMT is present in both the nucleus and the cytoplasm

The core of the cytoplasmic capping complex consists of CE and a 5'-monophosphate kinase bound to adjacent SH3 domains of adapter protein Nck1 (11). From results in (5), we knew that recapped 5' ends are methylated; however, the responsible methyltransferase remained to be identified. The most likely candidate was RNA guanine-7 methyltransferase (RNMT or cap methyltransferase). RNMT is highly specific for unmethylated caps (24), and there was evidence in (5) for a cytoplasmic pool of this enzyme.

Immunofluorescence showed the expected nuclear staining for RNMT but also revealed the presence of RNMT throughout the cytoplasm (Figure 1A). RNMT staining concentrated in the perinuclear region, and varying degrees

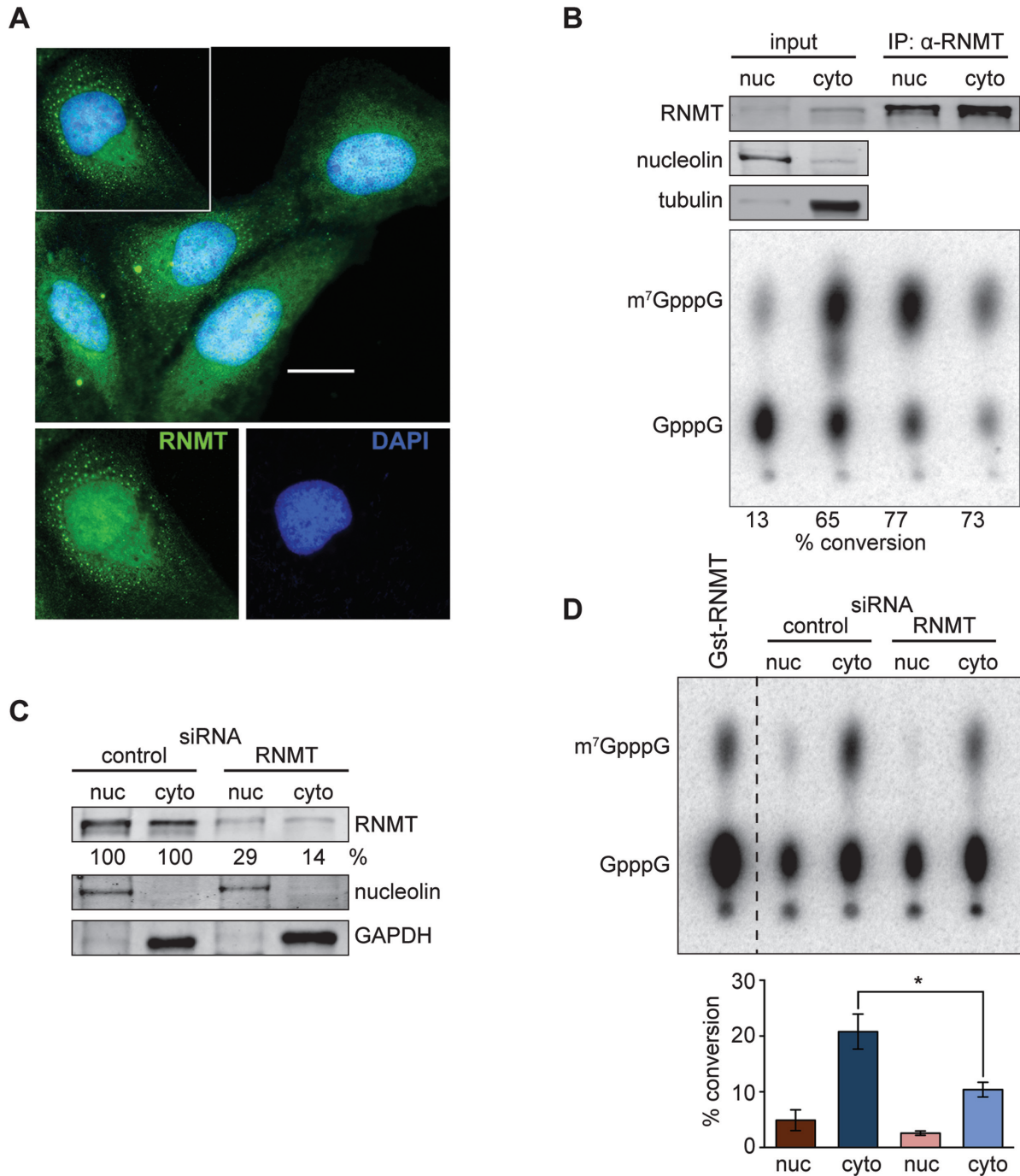


**Figure 1.** Identification of a cytoplasmic pool of RNMT. (A) U2OS cells were fixed with methanol, stained with rabbit anti-RNMT antibody and DAPI, co-stained with Alexa Fluor 488-labeled anti-rabbit antibody, and imaged with a fluorescence microscope. The scale bar indicates 15  $\mu$ m. (B) HEK293 cells were fractionated into nuclear and cytoplasmic extracts. These were analyzed directly by western blotting (lanes 1 and 2) or recovered by immunoprecipitation with rabbit anti-RNMT prior to western blotting (lanes 3 and 4). The same extracts were analyzed by cap methyltransferase activity assay, in which equal mass amounts of extract were incubated with S-adenosylmethionine and a 32-nt long [<sup>32</sup>P]cap-labeled RNA. The reaction products were digested with P1 nuclease prior to separation by PEI cellulose TLC and visualization by phosphorimager. The identity of each P1 digestion product was determined by comparison to known standards run on the same plate. (C) U2OS cells were transfected with control or RNMT siRNA, and the extent of knockdown was determined by western blotting and is shown quantitatively below the gel. (D) Cap methyltransferase activity was determined for nuclear and cytoplasmic extracts from control and RNMT knockdown cells. A representative autoradiogram is shown in the upper panel, and the quantified results from three independent experiments (mean  $\pm$  SEM) is shown in the lower panel. The asterisk (\*) indicates  $P < 0.05$  by ratio paired  $t$ -test.

of punctate cytoplasmic staining were seen in every cell we examined. Cytoplasmic RNMT staining has also been reported for U2OS, A431 and U251 cells in the Cell Atlas (25) and is independent of whether cells are fixed with methanol (Figure 1A) or with formaldehyde (Supplementary Figure S1). A pattern of punctate cytoplasmic staining was also seen previously for CE (5). Western blotting of nuclear and cytoplasmic extracts and immunoprecipitation with anti-RNMT antibody provided further evidence for a cytoplasmic pool of RNMT (Figure 1B, upper panels). Phosphorylation of RNMT on threonine at position 77 interferes with RNMT binding to the KPNA2 subunit of importin- $\alpha$  (26), and while it was conceivable this might be responsible for the observed cytoplasmic pool, we saw no evidence for this by western blotting of immunoprecipitated RNMT with anti-phosphothreonine antibody (Supplementary Figure S2).

The functionality of cytoplasmic RNMT was evaluated by the ability of protein present in crude extract and immunoprecipitated RNMT to methylate G-capped RNA. In Figure 1B, nuclear and cytoplasmic extracts (lanes 1 and 2) or immunoprecipitated nuclear and cytoplasmic RNMT (lanes 3 and 4) were incubated with [<sup>32</sup>P]G-capped RNA and S-adenosylmethionine. The reaction products were digested with P1 nuclease, separated by PEI cellulose thin layer chromatography (TLC) and visualized by phosphorimager. GpppG and m<sup>7</sup>GpppG were identified by comparing their mobilities to known standards. Cytoplasmic extract contained unexpectedly robust RNMT activity, and the activity of immunoprecipitated protein confirmed both the functional nature of this protein and the broad subcellular distribution seen in Figure 1A.

RNA interference provided additional confirmation for the existence of a cytoplasmic pool of RNMT. In Figure 1C, U2OS cells were transfected with control or RNMT siRNAs. Western blotting confirmed parallel loss of RNMT from nuclear and cytoplasmic fractions, and this was matched by a parallel decrease in nuclear and cytoplasmic RNMT activity (Figure 1D). Together, the results in Figure 1 demonstrate that cells have a pool of cytoplasmic RNMT that is as functional as its nuclear counterpart in catalyzing cap methylation.

### RNMT is a component of the cytoplasmic capping complex

In order to methylate recapped transcripts, RNMT must either be associated with the cytoplasmic capping complex or have some way of targeting these after guanylylation. As a first test, we examined the recovery of endogenous protein with the cytoplasmic capping complex. Gel filtration performed in (11) showed that the cytoplasmic capping complex eluted just past the void volume of a calibrated Sephacryl S-200 column. The stored fractions were re-examined by western blotting with antibodies to RNMT, CE and Nck1 (Figure 2A). RNMT co-eluted with CE and Nck1, and like CE, was not detected in later fractions. This is consistent with the cytoplasmic pool of RNMT being restricted to the cytoplasmic capping complex. Cap methyltransferase activity tracked with the intensity of western blot staining for all three proteins (Figure 2B), indicating that RNMT associated with the cytoplasmic capping com-

plex is functional. Next, HEK293 cells were transfected with plasmids expressing cytoplasmically restricted CE or a control protein consisting of multiple MS2 stem-loop binding sites, each with a biotinylation tag (bio-cCE or MS2-bio, (11)) (Figure 2C). The selective streptavidin-bead recovery of both Nck1 and RNMT with cCE provided additional evidence for RNMT as a component of the cytoplasmic capping complex.

It was conceivable that RNMT might join the cytoplasmic capping complex by binding to the first SH3 domain or the SH2 domain of Nck1. However, RNMT lacks a proline-rich sequence necessary for SH3 domain binding, and while it does have a potential tyrosine phosphorylation site at Y10 (20), the sequence surrounding this tyrosine residue is incompatible with binding to the SH2 domain of Nck1 (27). Additionally, we saw no evidence for tyrosine phosphorylation by western blotting of immunoprecipitated cytoplasmic RNMT with anti-phosphotyrosine antibody. We therefore sought to determine if RNMT is recruited to the complex through a direct interaction with CE or by binding to some other protein on one of the available domains of Nck1. In nuclear capping, CE and RNMT are brought together at the phosphorylated C-terminal domain of RNA polymerase II (28). The identification of m<sup>7</sup>G-capped tRNA precursors (29) suggested that CE and RNMT may interact in a manner independent of RNA polymerase II. Direct binding would be the most straightforward explanation, but there are conflicting reports as to whether RNMT and CE interact with one another (30,31). To examine this, GST-RNMT and His-CE were expressed in *Escherichia coli* (Figure 2D), and these proteins were incubated prior to recovery on glutathione agarose. The recovery of CE with GST-RNMT but not with a GST control (Figure 2E) indicates that RNMT can interact directly with CE.

We next sought to identify the portion of RNMT that mediates its *in vivo* interaction with the cytoplasmic capping complex using an approach similar to that in (21) to characterize functional domains of RNMT. Plasmids were generated that express FLAG-tagged forms of the full-length (FL) protein, the N-terminal 120 amino acids, and the catalytic C-terminal domain spanning amino acids 121–476. The subcellular distribution of each of these proteins was determined prior to their use in mapping CE-interacting sites (Supplementary Figure S3). Although RNMT(1–120) was reported to contain several nuclear localization sequences (32), this protein was found predominantly in the cytoplasmic fraction. RNMT(121–476) was both nuclear and cytoplasmic. Each of these plasmids was transfected into HEK293 cells alongside a plasmid expressing bio-CE, and cytoplasmic extracts were recovered on streptavidin beads (Figure 2F). FL RNMT and the portion spanning residues 121–476 were recovered with bio-cCE, but the N-terminal portion spanning residues 1–120 was not. Thus, residues within the C-terminal methyltransferase domain are responsible for recruitment of RNMT into the cytoplasmic capping complex. Taken together, the results in Figures 1 and 2 show that cells contain a functional cytoplasmic pool of RNMT, that the entirety of cytoplasmic RNMT is associated with the cytoplasmic capping complex, and that it is recruited to the complex by direct binding to CE.

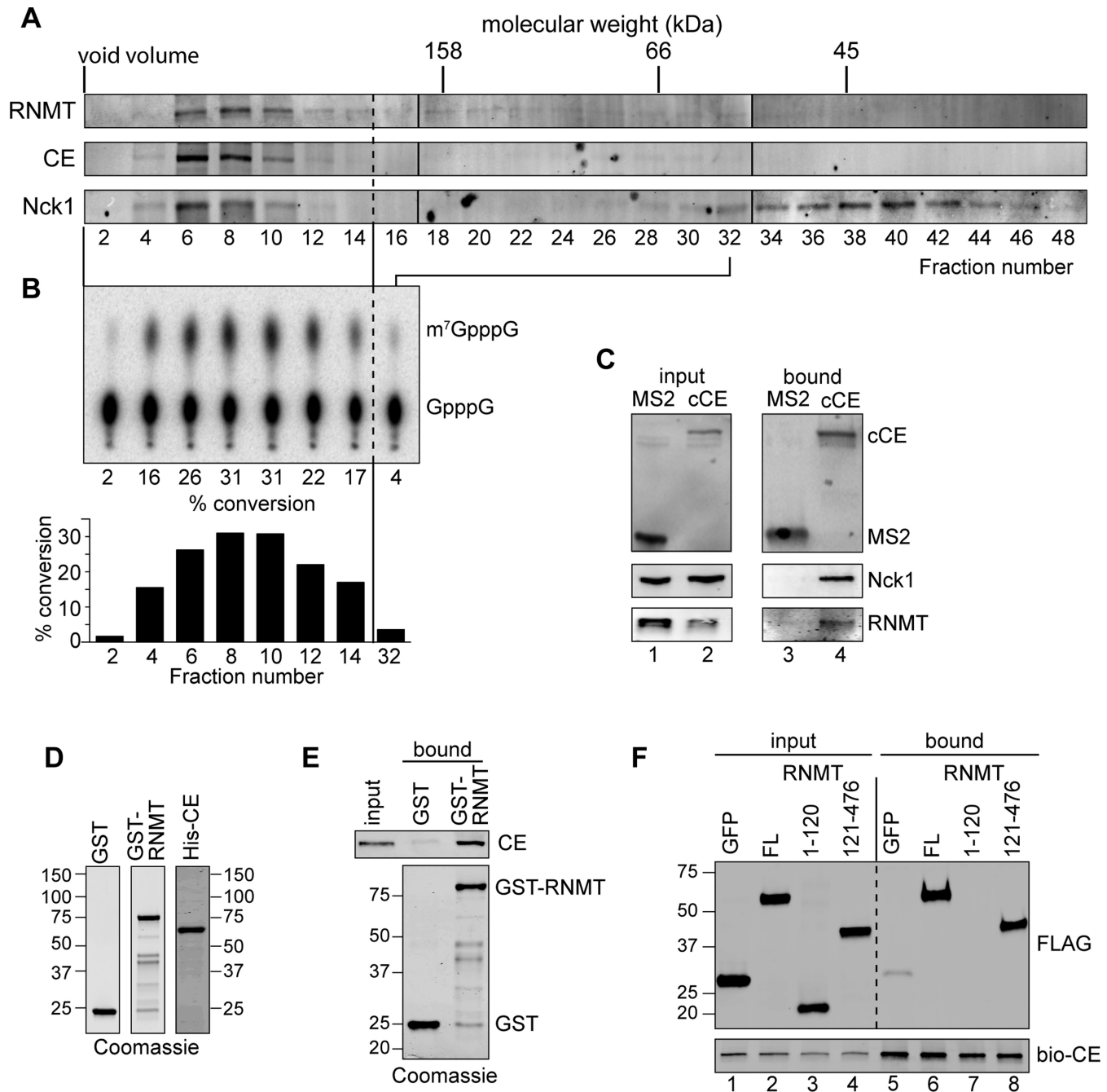


**Figure 2.** RNMT is a component of the cytoplasmic capping complex and binds to CE through its C-terminal catalytic domain. **(A)** Stored Sephacryl S-200 column fractions from (11) were analyzed by western blotting for RNMT, CE and Nck1. **(B)** Fractions 2–14 and fraction 34, which corresponds in size to monomeric RNMT, were analyzed for cap methyltransferase activity. The percent conversion of unmethylated to methylated caps is shown graphically beneath the autoradiogram. **(C)** HEK293 cells were transfected with plasmids expressing two MS2 binding domains or a cytoplasmically-restricted form of CE, each of which is coupled to a biotinylation tag (11). Cytoplasmic extracts were recovered on streptavidin beads, and the input (lanes 1 and 2) and bound (lanes 3 and 4) samples were analyzed by western blotting with streptavidin (upper panels) or antibodies to Nck1 and RNMT (lower panels). **(D)** GST, GST-RNMT and His-CE were expressed in *Escherichia coli*, purified on glutathione-Sepharose or cobalt-agarose beads as appropriate and analyzed by SDS-PAGE. Shown are Coomassie Blue stained gels of purified proteins. **(E)** Mixtures containing 1  $\mu$ g His-CE and 5  $\mu$ g GST or GST-RNMT were prepared for subsequent GST pull-down assay. Because His-CE runs at the same size as GST-RNMT, its recovery was monitored by western blotting with anti-CE antibody. This is shown in the upper panel, where 2% of input and 90% of bound protein was analyzed for CE recovery with GST-RNMT. The lower panel is a Coomassie-stained gel containing 10% of bead-bound protein. **(F)** HEK293 cells were co-transfected with plasmids expressing CE with an N-terminal biotinylation tag (bio-CE) and FLAG-GFP (lanes 1 and 5) or FLAG-tagged forms of full-length RNMT (FL, lanes 2 and 6), the N-terminal portion of RNMT (1–120, lanes 3 and 7), or the C-terminal portion of RNMT (121–476, lanes 4 and 8). Cytoplasmic extracts recovered on streptavidin beads were analyzed by western blotting with an anti-FLAG antibody and streptavidin.

### Proximity-dependent biotinylation identifies RNMT and RAM as constituents of the cytoplasmic capping complex

Proximity-dependent biotinylation (BioID) is a powerful tool for *in vivo* detection of proteins that are juxtaposed within a larger complex (33). Importantly, it reduces the possibility of scoring non-specific interactions that can occur during cell fractionation and allows for identification of transient *in vivo* interactions that may be lost during traditional pulldown methods. BirA\* and Myc tags were added to the N-terminus of a form of CE that is restricted to the cytoplasm due to loss of its NLS and addition of the HIV Rev NES (BirA\*-cCE) (5). A parallel construct expressing Myc-tagged BirA\* without CE was used as a control for non-specific biotinylation. Plasmids expressing each of these proteins and FLAG-RNMT were transfected into HEK293 cells and cultured for 14 h in medium containing 0, 5 or 25  $\mu$ M biotin. Cytoplasmic extracts recovered on streptavidin beads were then analyzed by western blotting.

Cytoplasmic BirA\* and BirA\*-cCE were expressed regardless of biotin supplementation (Figure 3A, upper left panel), and their recovery on streptavidin beads shows each of these was biotinylated only when the cells were supplemented with biotin (Figure 3A, upper right panel). The recovery of Nck1 from cells expressing BirA\*-cCE but not BirA\* (compare lanes 8 and 9 with lanes 11 and 12) confirmed the utility of BioID for identifying components of the cytoplasmic capping complex, and the selective recovery of RNMT confirmed its identification as a component of the cytoplasmic capping complex. In addition, the absence of GAPDH confirmed the specific biotin labeling of proteins in the cytoplasmic capping complex. RNMT functions as a heterodimer with a 118 amino acid protein termed RNMT-activating mini-protein (RAM) (21). RAM was present in the input cytoplasmic extract and, like Nck1 and RNMT, was selectively recovered with BirA\*-cCE.

The preceding results do not indicate if RNMT and RAM were biotinylated by BirA\*-cCE or if their recovery was secondary to their interaction with proteins of the cytoplasmic capping complex. To address this, RNMT was recovered from the same extracts by anti-FLAG immunoprecipitation, and biotinylated proteins were visualized by streptavidin western blot (Figure 3B). The recovery of RAM with RNMT confirmed that these proteins interact with each other in the cytoplasm. Streptavidin western blotting showed RNMT was biotinylated by BirA\*-cCE, but RAM was not. This could be due either to RAM being too far away from the BirA\* moiety to be biotinylated or by its sequestration by RNMT. FLAG-RNMT also recovered a 30 kDa protein (solid dot) whose biotinylation by BirA\*-cCE identified this as an unknown constituent of the cytoplasmic capping complex that may contribute to cap methylation.

### Cytoplasmic RNMT is a heterodimer with RAM

The identification of RAM in the cytoplasmic capping complex suggested this RNMT cofactor might also be required for optimal cytoplasmic cap methyltransferase activity. Immunofluorescence confirmed the nuclear localization of RAM but also showed that RAM is in the cytoplasm and has perinuclear staining similar to that of RNMT

(Figure 4A). There was also evidence for punctate cytoplasmic staining in some cells, but this was less apparent than that for CE or RNMT. These results were complemented by western blot analysis of nuclear and cytoplasmic extracts of U2OS and HEK293 cells (Figure 4B). To determine if cytoplasmic RNMT is a heterodimer with RAM, nuclear and cytoplasmic extracts were immunoprecipitated with anti-RNMT antibody and probed for RAM (Figure 4C). The indistinguishable recovery of RAM from both fractions is consistent with the existence of cytoplasmic RNMT as a heterodimer with RAM. In (21), RAM knockdown suppressed cap methyltransferase activity present in whole-cell extracts. The experiment in Figure 4D and E compared cap methyltransferase activity in nuclear and cytoplasmic extracts of cells that were transfected with control or RAM siRNAs. RAM knockdown reduced the level of nuclear and cytoplasmic RAM to 18 and 30%, respectively (Figure 4D), and the impact on nuclear and cytoplasmic cap methyltransferase activity (Figure 4E) was almost identical to that seen with RNMT knockdown in Figure 1D. In agreement with results in (21), we also noted that RAM knockdown reduced the level of nuclear RNMT but had little impact on cytoplasmic RNMT. The reason for this difference is not known, but it may relate to differences in the complexes in which they reside.

### Methylation of cytoplasmic-capping targets

Cytoplasmic capping targets were originally identified by the appearance of uncapped transcripts in cells that overexpress a cytoplasmically restricted, inactive form of CE (6). A conceptually similar approach was used to determine if the same mRNAs undergo cytoplasmic cap methylation. Interference with cap methylation should result in the appearance of transcripts with an unmethylated guanylate 5' end whose presence would render these mRNAs susceptible to cap surveillance by one or more decapping enzymes (19,34). The corollary to this is that the cytoplasmic capping targets that remain when cap methylation is inhibited should all have m<sup>7</sup>G caps.

The development of a selective inhibitor of cytoplasmic cap methylation was based on results in Figure 2F showing that the C-terminal portion of RNMT mediates binding to CE. That portion of RNMT (spanning residues 121–476) also contains the active site and the RAM binding domain, but not the nuclear localization sequences. An inactive form of RNMT was created by changing the aspartic acid at position 203 in the SAM binding site to alanine (35). This particular site was chosen because it does not interfere with RAM binding (Supplementary Figure S4). As in our previous work (5), the addition of the HIV Rev NES resulted in a protein, termed  $\Delta$ N-RNMT (Figure 5A), that is almost entirely cytoplasmic (Figure 5D).

To be a functional inhibitor of cytoplasmic cap methylation,  $\Delta$ N-RNMT should be incorporated into the cytoplasmic capping complex and bind to RAM such that the displaced endogenous RNMT is less active. The incorporation of  $\Delta$ N-RNMT was examined by proximity-dependent biotinylation (Figure 5B) using cells transfected with plasmids expressing  $\Delta$ N-RNMT and BirA\* or BirA\*-cCE. The selective biotinylation of  $\Delta$ N-RNMT by BirA\*-cCE but

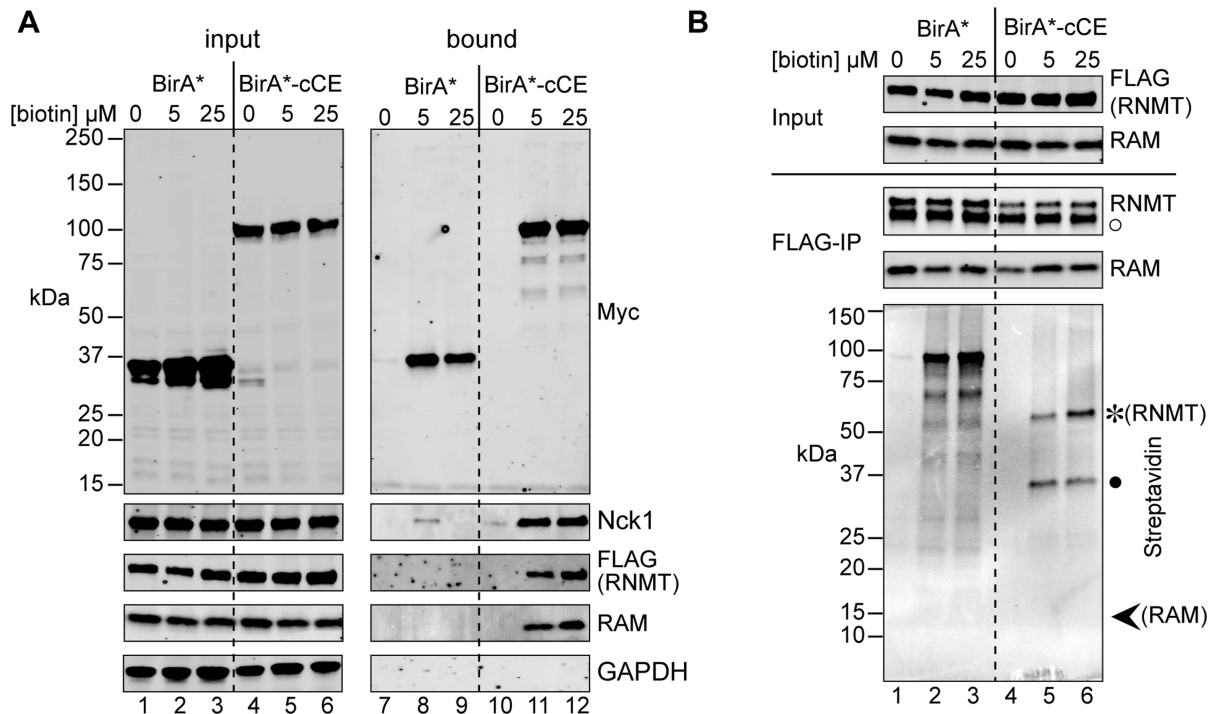


**Figure 3.** Proximity-dependent biotinylation identifies RNMT and RAM as components of the cytoplasmic capping complex. (A) HEK293 cells were co-transfected with plasmids expressing Myc-tagged BirA\* or BirA\*-cCE together with FLAG-RNMT. Cells were cultured in medium containing 0, 5 or 25  $\mu\text{M}$  biotin, and cytoplasmic extracts recovered on streptavidin beads were analyzed by western blotting with antibodies to Myc (BirA\* and BirA\*-cCE), FLAG (RNMT), Nck1, RAM and GAPDH. (B) The cytoplasmic extracts from (A) were immunoprecipitated with anti-FLAG antibody. For comparison, the input samples from (A) are reproduced at the top of (B). Western blotting with anti-RNMT and anti-RAM confirmed their recovery with anti-FLAG immunoprecipitation. The open circle (○) in the RNMT western blot indicates IgG heavy chain. Biotinylated proteins recovered with anti-FLAG immunoprecipitation were identified by western blotting with streptavidin. RNMT is indicated with an asterisk (\*), and an unknown 30-kDa protein is indicated with a filled circle (●).

not BirA\* alone confirmed the incorporation of this modified protein into the cytoplasmic capping complex.  $\Delta\text{N}$ -RNMT also retains the ability to bind RAM (Supplementary Figure S4), and we confirmed that  $\Delta\text{N}$ -RNMT overexpression reduces the enzymatic activity of endogenous RNMT in cytoplasmic extracts (Figure 5C). It was conceivable that  $\Delta\text{N}$ -RNMT overexpression could interfere with nuclear cap methylation by changing the overall subcellular distribution of RAM. This proved not to be the case. In the experiment in Figure 5D, triplicate cultures of U2OS cells were transfected with empty vector or  $\Delta\text{N}$ -RNMT plasmid, together with a plasmid expressing EGFP.  $\Delta\text{N}$ -RNMT had no impact on the levels or nucleocytoplasmic distribution of RAM or of RNMT, thus confirming its impact should be limited to cytoplasmic cap methylation.

Cytoplasmic RNA from the same cells was analyzed by RT-qPCR (Figure 5E) for quantitative changes in two control mRNAs (RPLP0 and STRN4) and six recapping targets (POLR2B, ZNF207, VDAC3, EXOSC2, MAPK1 and STAT3), each of which accrues uncapped forms when cytoplasmic CE is inhibited. Because  $\Delta\text{N}$ -RNMT does not affect levels of nuclear RNMT or RAM, it should not interfere with nuclear cap methylation of RPLP0 and STRN4, and this indeed was the case. In contrast,  $\Delta\text{N}$ -RNMT expression resulted in a statistically significant decrease in the steady-state levels of POLR2B, ZNF207 and VDAC3

mRNA. The levels of the other target mRNAs also decreased but not to a degree that was statistically significant.

If mRNAs with unmethylated caps were degraded, the remainder should all have  $\text{m}^7\text{G}$  caps. This was examined by their recovery on immobilized eIF4E, which is highly selective for RNAs with properly methylated caps (17). We reasoned that if the entire population of each remaining transcript has an  $\text{m}^7\text{G}$  cap,  $\Delta\text{N}$ -RNMT expression should have no impact on the eIF4E-based recovery. However, if this population included G-capped transcripts, the amount of each mRNA recovered on eIF4E should be lower for cells expressing  $\Delta\text{N}$ -RNMT compared to vector control. Prior to binding to eIF4E, each preparation was spiked with G-capped luciferase RNA, and input and bound RNAs were quantified by RT-qPCR. As expected, there was minimal binding of G-capped luciferase RNA (Figure 5F), and eIF4E bound approximately 20% of  $\text{m}^7\text{G}$ -capped EGFP mRNA expressed from the co-transfection control plasmid. While the percent recovery on eIF4E differed for each of the control and target mRNAs, there was no difference in cap status between the two treatment groups, indicating that only mRNAs with  $\text{m}^7\text{G}$  caps remain when cytoplasmic cap methylation is inhibited.

## DISCUSSION

The discovery of cytoplasmic capping grew out of the observation that metastable  $\beta$ -globin decay intermediates have

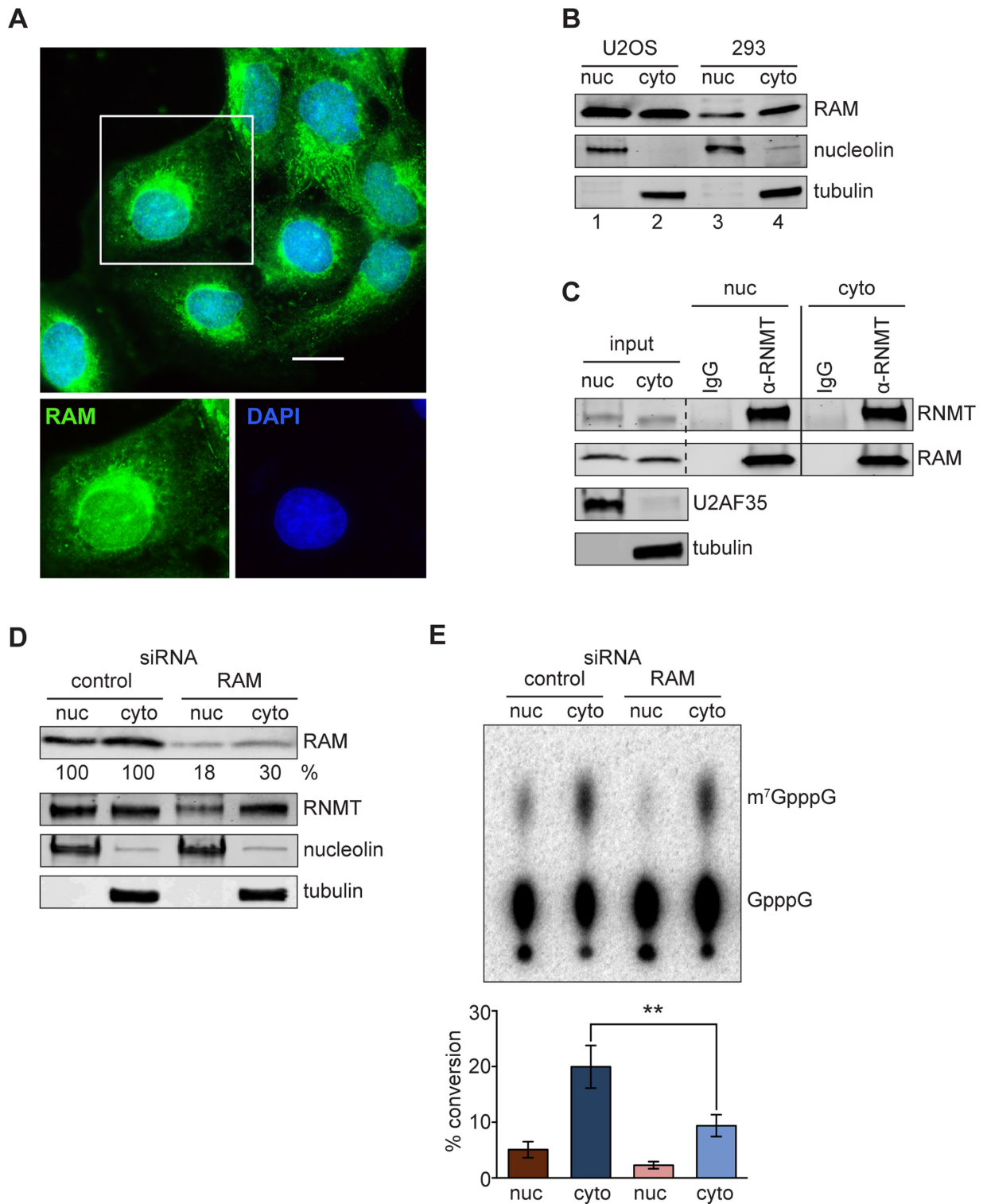


**Figure 4.** Identification of RAM as a cofactor that activates cytoplasmic RNMT. (A) U2OS cells were prepared and imaged as in Figure 1A, except that rabbit anti-RAM antibody was used for staining. The scale bar indicates 10  $\mu$ m. (B) Cytoplasmic and nuclear extracts from U2OS and HEK293 cells were examined for the presence of RAM by western blotting with rabbit anti-RAM antibody. Nucleolin and tubulin were also examined as controls for cross contamination between nuclear and cytoplasmic extracts. (C) Nuclear and cytoplasmic extracts of U2OS cells were immunoprecipitated with control IgG or anti-RNMT antibody and analyzed by western blotting for recovery of RAM and RNMT. The input samples were also probed for tubulin and U2AF35 as controls for cross contamination. (D) U2OS cells were transfected with control or RAM siRNAs and separated into nuclear and cytoplasmic fractions. The effectiveness of knockdown was determined by western blotting with anti-RAM antibody, and quantified results are shown beneath the upper panel. The same samples were also analyzed by western blotting for RNMT, nucleolin and tubulin. (E) Cap methyltransferase activity of nuclear and cytoplasmic extracts from cells that were transfected with control or RAM-specific siRNAs was determined as in Figure 1D with the results from three independent experiments (mean  $\pm$  SEM) shown beneath the autoradiogram. The double asterisk (\*\*) indicates  $P < 0.01$  by ratio paired *t*-test.

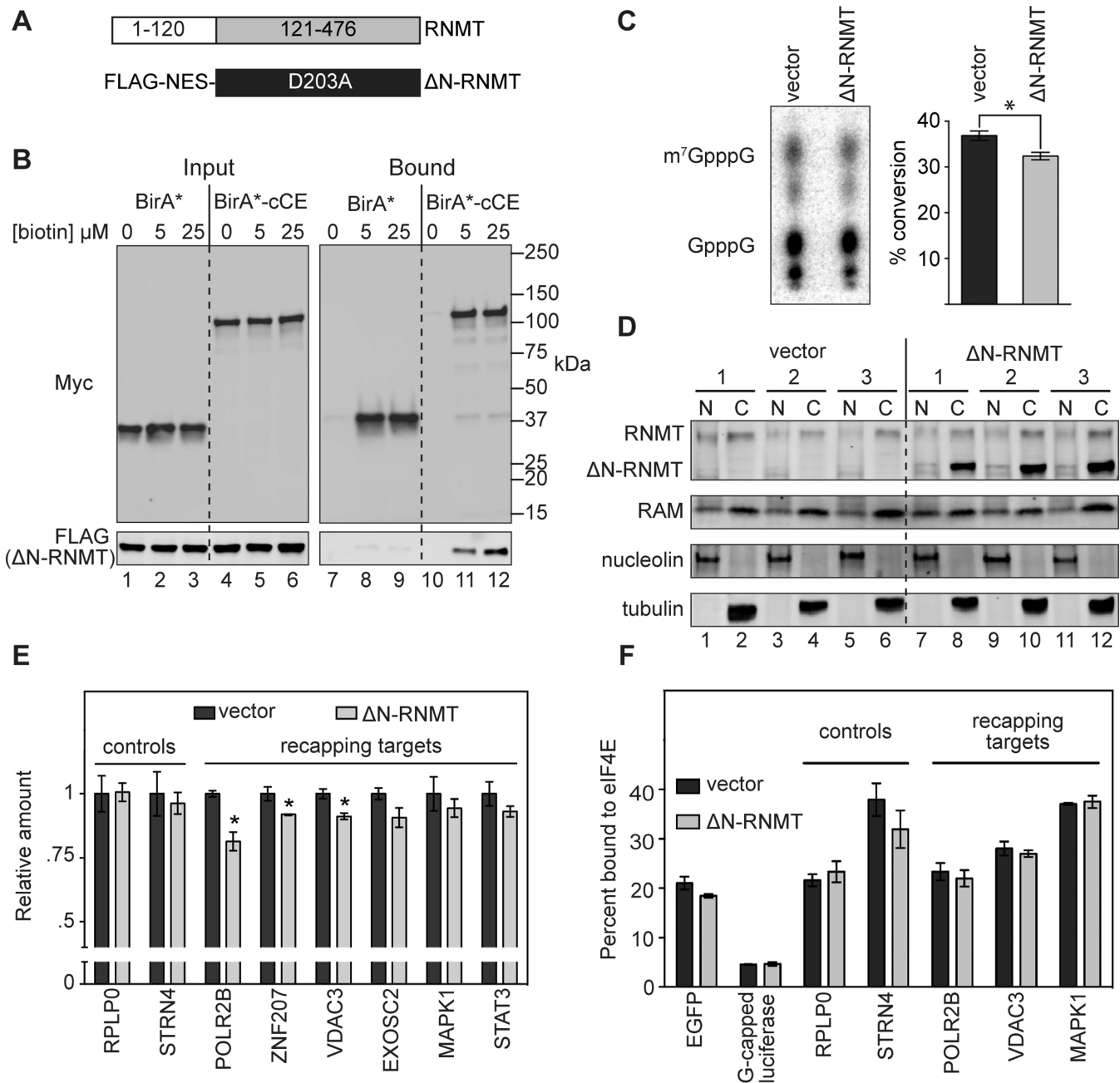


**Figure 5.** Levels of recapped mRNAs decline when cytoplasmic cap methylation is inhibited. (A) Schematic showing the relationship of  $\Delta$ N-RNMT to the native protein and the modifications that were made to create this inhibitor of cytoplasmic cap methylation. (B) Cells were transfected as in Figure 3A with plasmids expressing FLAG-tagged  $\Delta$ N-RNMT and Myc-tagged BirA\* or BirA\*-cCE and cultured with indicated biotin concentrations. Cytoplasmic protein recovered on streptavidin beads was analyzed by western blotting with antibodies to the Myc and FLAG epitopes. (C) Cap methyltransferase activity was determined for cytoplasmic extracts of HEK293 cells transfected with an empty vector or a plasmid expressing  $\Delta$ N-RNMT. A representative autoradiogram is shown in the left panel, and the quantified results from three independent experiments (mean  $\pm$  SEM) is shown in the right panel. The asterisk (\*) indicates  $P < 0.05$  by unpaired two-tailed  $t$ -test. (D) Triplicate cultures of U2OS cells were co-transfected with a plasmid expressing EGFP and either empty vector or plasmid expressing  $\Delta$ N-RNMT. Nuclear and cytoplasmic extracts were analyzed by western blotting with antibodies to RNMT, RAM, nucleolin and tubulin. (E) Cytoplasmic RNA recovered from each of the transfectants in (D) was analyzed by RT-qPCR for two control mRNAs (RPLP0 and STRN4) and six of the cytoplasmic capping targets identified in (6) (POLR2B, ZNF207, VDAC3, EXOSC2, MAPK1, STAT3). Relative abundances were normalized to spiked-in luciferase RNA and to the non-recapping control mRNA BOP1. Shown is the mean  $\pm$  SEM ( $n = 3$ ). The asterisk (\*) indicates  $P < 0.05$  by unpaired two-tailed  $t$ -test. (F) The RNAs analyzed in (E) were spiked with G-capped luciferase RNA and incubated with GST-eIF4E bound magnetic beads. Input and bound RNAs were quantified by RT-qPCR, and the results were plotted as percent bound (normalized to input). Paired measurements were used for the vector control. For each mRNA there was no statistically significant difference in recovery between treatment groups.

a cap structure that is indistinguishable from the m<sup>7</sup>G caps on mRNAs that are capped in the nucleus (4,5). Results in (6) showed that cytoplasmic capping targets cycle between capped and uncapped states (cap homeostasis) and that recapping serves to maintain the stability of a portion of these targets and the translatability of another portion. Because cytoplasmic capping targets are polyadenylated (10), recapping is all that is necessary to restore these uncapped transcripts from a non-translating state to a translating state. Three sequential reactions are needed for cytoplasmic capping: conversion of a 5'-monophosphate end of a decapped RNA to a 5'-diphosphate, addition of GMP, and methylation to generate the m<sup>7</sup>G cap structure. The first two reactions are carried out by a 5'-monophosphate kinase and CE that are brought together in a single complex by binding to the second and third SH3 domains, respectively, of the cytoplasmic adapter protein Nck1 (11). Here we identify RNMT as the third enzyme of the cytoplasmic capping metabolon.

RNMT heterodimerizes with RAM, and both were originally classified as nuclear proteins. Initial evidence for a cytoplasmic pool of RNMT was described in (5), but because RNMT did not co-sediment with CE, it was not examined further. Structural studies in (24) showing that RNMT:RAM is specific for unmethylated caps led us to revisit cytoplasmic RNMT, and results in Figure 1 confirmed the existence of a cytoplasmic pool. Furthermore, the loss of nuclear and cytoplasmic cap methyltransferase activity following RNMT knockdown confirmed its identity as the major, if not only, cap methyltransferase in the cell. While it was conceivable that the cytoplasmic pool of RNMT (and RAM) results from loss of the nuclear envelope during mitosis, their cytoplasmic immunofluorescence staining in non-dividing cells and cytoplasmic abundance by subcellular fractionation suggest otherwise.

Evidence for RNMT as a component of the cytoplasmic capping complex was provided by co-precipitation experiments (Figure 2C and E) and by the gel filtration experiment in Figure 2A where RNMT, CE and Nck1 eluted as a single entity. The fact that neither CE nor RNMT was present in later fractions suggests the entirety of their cytoplasmic populations is present in this complex. This was reinforced by the elution of cap methyltransferase activity in the same fractions as CE and Nck1 (Figure 2B) but not in a later fraction corresponding to the size of monomeric RNMT. Additional support for cytoplasmic cap methylation came from the identification of a cytoplasmic pool of RAM. RAM is a cofactor that dramatically stimulates cap methyltransferase activity (21). Initial evidence for the presence of RAM in the cytoplasmic capping complex came from proximity-dependent biotinylation with BirA\*-tagged cCE (Figure 3). In this experiment, RNMT was biotinylated, but RAM was not, suggesting that RAM is either sequestered by RNMT or is sufficiently far from the BirA\* moiety that it was not biotinylated. The existence of cytoplasmic RAM was confirmed by immunofluorescence (Figure 4A), biochemical fractionation (Figure 4B), and recovery with cytoplasmic RNMT (Figure 4C). Importantly, the impact of RAM knockdown was almost identical to that of RNMT knockdown (compare Figures 1D and 4E), thus

confirming both its presence in the cytoplasm and its obligate role in cytoplasmic cap methylation.

The left panel of Figure 6 shows a model of our current understanding of the organization of the cytoplasmic capping complex, with the 5' kinase and CE bound to adjacent SH3 domains of Nck1. RNMT lacks a proline-rich sequence needed for binding to Nck1, and our inability to visualize any interaction between these proteins ruled out the first SH3 domain as the RNMT binding site. Although PhosphoSite (36) identified three tyrosine phosphorylation sites on RNMT, none of these matched the sequence needed for binding to the SH2 domain of Nck1 (27), and we saw no evidence for tyrosine phosphorylation of RNMT by western blotting of immunoprecipitated protein with anti-phosphotyrosine antibodies. This suggested RNMT was recruited by direct interaction with CE or some other protein. An earlier report described evidence for a direct interaction between CE and RNMT (30), and this was confirmed with purified recombinant proteins (Figure 2E). RNMT has been operationally divided into two domains spanning amino acids 1–120 and 121–476 (35). RNMT(1–120) has several nuclear localization sequences and mediates the recruitment of RNMT to transcription initiation sites (31). RNMT(121–476) contains the active site and RAM-binding residues (24). This latter domain mediates RNMT binding to CE (Figure 2F), and a direct association between these proteins is consistent with 5' end capping of pre-tRNAs (29).

Cells have surveillance mechanisms that degrade improperly capped transcripts (18), and despite repeated attempts we were never able to detect unmethylated, G-capped forms of cytoplasmic capping targets. This contrasted with our ability to detect uncapped forms of the same mRNAs (6). We used the loss of improperly capped target mRNAs as *in vivo* evidence for cytoplasmic cap methylation. As noted above, the portion of residues spanning 121–476 contains the active site and RAM binding domain and mediates RNMT binding to CE. Mutating a single amino acid (D203A) in the SAM binding site and adding the HIV Rev NES generated an inactive protein ( $\Delta$ N-RNMT) that is restricted to the cytoplasm but still able to bind RAM and be incorporated into the cytoplasmic capping complex. Over-expressed  $\Delta$ N-RNMT competes with endogenous RNMT for binding to the cytoplasmic capping complex (Figures 5B and 6, right panel) and to RAM (Supplementary Figure S4), reducing the overall cap methylation activity in the cytoplasm (Figure 5C). Importantly,  $\Delta$ N-RNMT has no impact on nuclear RNMT or RAM (Figure 5D). Consistent with cellular surveillance for improperly capped transcripts,  $\Delta$ N-RNMT reduced the steady-state level of each of six recapping targets but had no effect on two control mRNAs that are not subject to cytoplasmic recapping (Figure 5E). Although the degrees of loss were modest, they are consistent with results in (6) showing only a subfraction of any given recapping target is subject to cap homeostasis. The selective loss of improperly capped transcripts was confirmed by binding onto eIF4E, which is highly selective for methylated versus unmethylated caps (17) (Figure 5F). This approach would have shown a difference in recovery between treatment groups if RNA from  $\Delta$ N-RNMT-expressing cells contained transcripts with improperly methylated caps. The

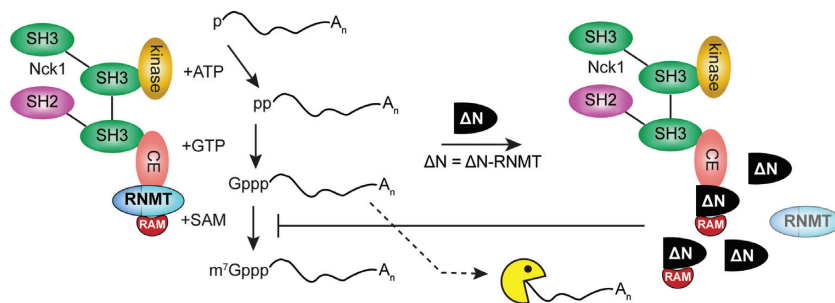


**Figure 6.** Model for the interaction of RNMT with the cytoplasmic capping complex. The left panel shows the organization of known components of the cytoplasmic capping complex. The 5'-kinase that generates a diphosphate capping substrate binds to the second SH3 domain of Nck1, and CE binds to the third SH3 domain. RNMT:RAM binds directly to CE, with binding mediated by sequences in the C-terminal portion spanning residues 121–476. In the right panel, cytoplasmic cap methylation is inhibited by overexpression of  $\Delta N$ -RNMT. This displaces endogenous RNMT from the cytoplasmic capping complex and also sequesters cytoplasmic RAM without altering nuclear or cytoplasmic levels of RNMT or RAM.

fact that no such difference was observed (Figure 5F) confirmed that the reduction in recapping targets was due to loss of unmethylated transcripts as a consequence of  $\Delta N$ -RNMT inhibition of cytoplasmic cap methylation.

This observation has implications for regulation. Phosphorylation of RAM leads to its ubiquitination and degradation by the proteasome and an overall decrease in cellular cap methyltransferase activity (22). At this point in time it is unclear whether a similar process also applies to the cytoplasmic pool, but one can envision how loss of cytoplasmic RAM could result in downregulation of a portion of cytoplasmic capping targets. This also has implications for proteome complexity. Most of the cytoplasmic capping targets identified in (6) have downstream CAGE tags, and we showed in (9) that recapped ends map to the vicinity of these. These mRNAs also have a statistically higher representation of downstream in-frame start codons, and altering cytoplasmic cap methylation has the potential to affect production of N-terminally truncated proteins from recapped mRNAs.

## SUPPLEMENTARY DATA

Supplementary Data are available at NAR Online.

## ACKNOWLEDGEMENTS

We wish to thank Juan Alfonzo and members of the Schoenberg lab for their input and helpful comments.

## FUNDING

National Institutes of Health (NIH) Grant [GM084177 to D.R.S.]; NIH Training Grant [GM08512 to Ohio State University]; Ohio State University Center for RNA Biology Pre-doctoral Fellowship (to J.B.T.); American Heart Association Postdoctoral Fellowship [13POST172700021 to C.M.]; Ohio State University Comprehensive Cancer Center Pelotonia Undergraduate Fellowship (to A.J.G.). Funding for open access charge: NIH Grant [GM084177].

*Conflict of interest statement.* None declared.

## REFERENCES

- Ramanathan, A., Robb, G.B. and Chan, S.H. (2016) mRNA capping: biological functions and applications. *Nucleic Acids Res.*, 7511–7526.
- Stevens, A., Wang, Y., Bremer, K., Zhang, J., Hoepfner, R., Antoniou, M., Schoenberg, D.R. and Maquat, L.E. (2002) Beta-globin mRNA decay in erythroid cells: UG site-preferred endonucleolytic cleavage that is augmented by a premature termination codon. *Proc. Natl. Acad. Sci. U.S.A.*, 99, 12741–12746.
- Mascarenhas, R., Dougherty, J.A. and Schoenberg, D.R. (2013) SMG6 cleavage generates metastable decay intermediates from nonsense-containing  $\beta$ -globin mRNA. *PLoS One*, 8, e74791.
- Lim, S.K. and Maquat, L.E. (1992) Human beta-globin mRNAs that harbor a nonsense codon are degraded in murine erythroid tissues to intermediates lacking regions of exon I or exons I and II that have a cap-like structure at the 5' termini. *EMBO J.*, 11, 3271–3278.
- Otsuka, Y., Kedersha, N.L. and Schoenberg, D.R. (2009) Identification of a cytoplasmic complex that adds a cap onto 5'-monophosphate RNA. *Mol. Cell. Biol.*, 29, 2155–2167.
- Mukherjee, C., Patil, D.P., Kennedy, B.A., Bakthavachalu, B., Bundschuh, R. and Schoenberg, D.R. (2012) Identification of cytoplasmic capping targets reveals a role for cap homeostasis in translation and mRNA stability. *Cell Rep.*, 2, 674–684.
- Fejes-Toth, K., Sotirova, V., Sachidanandam, R., Assaf, G., Hannon, G.J., Kapranov, P., Foissac, S., Willingham, A.T., Duttagupta, R., Dumais, E. and Gingeras, T.R. (2009) Post-transcriptional processing generates a diversity of 5'-modified long and short RNAs. *Nature*, 457, 1028–1032.
- Djebali, S., Davis, C.A., Merkel, A., Dobin, A., Lassmann, T., Mortazavi, A., Tanzer, A., Lagarde, J., Lin, W., Schlesinger, F. et al. (2012) Landscape of transcription in human cells. *Nature*, 489, 101–108.
- Kiss, D.L., Oman, K., Bundschuh, R. and Schoenberg, D.R. (2015) Uncapped 5' ends of mRNAs targeted by cytoplasmic capping map to the vicinity of downstream CAGE tags. *Febs Lett.*, 589, 279–284.
- Kiss, D.L., Oman, K.M., Dougherty, J.A., Mukherjee, C., Bundschuh, R. and Schoenberg, D.R. (2016) Cap homeostasis is independent of poly(A) tail length. *Nucleic Acids Res.*, 44, 304–314.
- Mukherjee, C., Bakthavachalu, B. and Schoenberg, D.R. (2014) The cytoplasmic capping complex assembles on adapter protein NCK1 bound to the proline-rich C-terminus of mammalian capping enzyme. *PLoS Biol.*, 12, e1001933.
- Srere, P.A. (1987) Complexes of sequential metabolic enzymes. *Annu. Rev. Biochem.*, 56, 89–124.
- Wu, F. and Minter, S. (2015) Krebs cycle metabolon: structural evidence of substrate channeling revealed by cross-linking and mass spectrometry. *Angew. Chem. Int. Ed. Engl.*, 54, 1851–1854.
- Ignatovich, A.V., Takagi, Y., Liu, Y., Nagata, K. and Ho, C.K. (2015) The messenger RNA decapping and recapping pathway in Trypanosoma. *Proc. Natl. Acad. Sci. U.S.A.*, 112, 6967–6972.
- Kumar, P., Hellen, C.U. and Pestova, T.V. (2016) Toward the mechanism of eIF4F-mediated ribosomal attachment to mammalian capped mRNAs. *Genes Dev.*, 30, 1573–1588.
- Marcotrigiano, J., Gingras, A.C., Sonenberg, N. and Burley, S.K. (1997) Cocystal structure of the messenger RNA 5' cap-binding protein (eIF4E) bound to 7-methyl-GDP. *Cell*, 89, 951–961.

17. Niedzwiecka,A., Marcotrigiano,J., Stepinski,J., Jankowska-Anyszka,M., Wyslouch-Cieszyńska,A., Dadlez,M., Gingras,A.C., Mak,P., Darzynkiewicz,E., Sonenberg,N. *et al.* (2002) Biophysical studies of eIF4E cap-binding protein: recognition of mRNA 5' cap structure and synthetic fragments of eIF4G and 4E-BP1 proteins. *J. Mol. Biol.*, **319**, 615–635.
18. Grudzien-Nogalska,E. and Kiledjian,M. (2017) New insights into decapping enzymes and selective mRNA decay. *Wiley Interdiscip. Rev. RNA*, **8**, e1379.
19. Jiao,X., Chang,J.H., Kilic,T., Tong,L. and Kiledjian,M. (2013) A mammalian pre-mRNA 5' end capping quality control mechanism and an unexpected link of capping to pre-mRNA processing. *Mol. Cell*, **50**, 104–115.
20. Aregger,M. and Cowling,V.H. (2017) Regulation of mRNA capping in the cell cycle. *RNA Biol.*, **14**, 11–14.
21. Gonatopoulos-Pournatzis,T., Dunn,S., Bounds,R. and Cowling,V.H. (2011) RAM/Fam103a1 is required for mRNA cap methylation. *Mol. Cell*, **44**, 585–596.
22. Grasso,L., Suska,O., Davidson,L., Gonatopoulos-Pournatzis,T., Williamson,R., Wasmus,L., Wiedlich,S., Peggie,M., Stavridis,M.P. and Cowling,V.H. (2016) mRNA cap methylation in pluripotency and differentiation. *Cell Rep.*, **16**, 1352–1365.
23. Yue,Z., Maldonado,E., Pillutla,R., Cho,H., Reinberg,D. and Shatkin,A.J. (1997) Mammalian capping enzyme complements mutant *Saccharomyces cerevisiae* lacking mRNA guanylyltransferase and selectively binds the elongating form of RNA polymerase. *Proc. Natl. Acad. Sci. U.S.A.*, **94**, 12898–12903.
24. Varshney,D., Petit,A.P., Bueren-Calabuig,J.A., Jansen,C., Fletcher,D.A., Peggie,M., Weidlich,S., Scullion,P., Pisljakov,A.V. and Cowling,V.H. (2016) Molecular basis of RNA guanine-7 methyltransferase (RNMT) activation by RAM. *Nucleic Acids Res.*, **44**, 10423–10436.
25. Thul,P.J., Åkesson,L., Wiking,M., Mahdessian,D., Geladaki,A., Ait Blal,H., Alm,T., Asplund,A., Björk,L., Breckels,L.M. *et al.* (2017) A subcellular map of the human proteome. *Science*, **356**, doi:10.1126/science.aal3321.
26. Aregger,M., Kaskar,A., Varshney,D., Fernandez-Sanchez,M.E., Inesta-Vaquera,F.A., Weidlich,S. and Cowling,V.H. (2016) CDK1-cyclin B1 activates RNMT, coordinating mRNA cap methylation with G1 phase transcription. *Mol. Cell*, **61**, 734–746.
27. Frese,S., Schubert,W.D., Findeis,A.C., Marquardt,T., Roske,Y.S., Stradal,T.E. and Heinz,D.W. (2006) The phosphotyrosine peptide binding specificity of Nck1 and Nck2 Src homology 2 domains. *J. Biol. Chem.*, **281**, 18236–18245.
28. Chiu,Y.L., Ho,C.K., Saha,N., Schwer,B., Shuman,S. and Rana,T.M. (2002) Tat stimulates cotranscriptional capping of HIV mRNA. *Mol. Cell*, **10**, 585–597.
29. Ohira,T. and Suzuki,T. (2016) Precursors of tRNAs are stabilized by methylguanosine cap structures. *Nat. Chem. Biol.*, **12**, 648–655.
30. Pillutla,R.C., Yue,Z., Maldonado,E. and Shatkin,A.J. (1998) Recombinant human mRNA cap methyltransferase binds capping enzyme/RNA polymerase II complexes. *J. Biol. Chem.*, **273**, 21443–21446.
31. Aregger,M. and Cowling,V.H. (2013) Human cap methyltransferase (RNMT) N-terminal non-catalytic domain mediates recruitment to transcription initiation sites. *Biochem. J.*, **455**, 67–73.
32. Shafer,B., Chu,C. and Shatkin,A.J. (2005) Human mRNA cap methyltransferase: alternative nuclear localization signal motifs ensure nuclear localization required for viability. *Mol. Cell Biol.*, **25**, 2644–2649.
33. Roux,K.J., Kim,D.I., Raida,M. and Burke,B. (2012) A promiscuous biotin ligase fusion protein identifies proximal and interacting proteins in mammalian cells. *J. Cell Biol.*, **196**, 801–810.
34. Song,M.G., Li,Y. and Kiledjian,M. (2010) Multiple mRNA decapping enzymes in mammalian cells. *Mol. Cell*, **40**, 423–432.
35. Saha,N., Schwer,B. and Shuman,S. (1999) Characterization of human, *Schizosaccharomyces pombe*, and *Candida albicans* mRNA cap methyltransferases and complete replacement of the yeast capping apparatus by mammalian enzymes. *J. Biol. Chem.*, **274**, 16553–16562.
36. Hornbeck,P.V., Chabra,I., Kornhauser,J.M., Skrzypek,E. and Zhang,B. (2004) PhosphoSite: a bioinformatics resource dedicated to physiological protein phosphorylation. *Proteomics*, **4**, 1551–1561.